JOURNAL OF MATERIALS SCIENCE 28 (1993) 5753–5758

The fractal dimension of grain-boundary fracture in high-temperature creep of heat-resistant alloys

M. TANAKA
Department of Mechanical Engineering, Mining College, Akita University, 1-1, Tegatagakuen-cho, Akita 010, Japan

The fractal dimension of the grain-boundary fracture in high-temperature creep was estimated by the vertical section method on several creep-ruptured specimens of the cobalt-nickel- and iron-based heat-resistant alloys. Grain-boundary microcracks linked to the fracture surface were also taken into account in the present analysis by the box-counting method. In the specimens containing many grain-boundary microcracks linked to the fracture surface, the fractal dimension of the grain-boundary fracture was larger in the scale range of more than about one grain-boundary length than in the scale range less than this length. Thus, there was a cross-over in the fractal dimension of the grain-boundary fracture at about one grain-boundary length in these specimens. In the specimens containing much fewer microcracks, there was no clear cross-over in the fractal dimension of the grain-boundary fracture with regard to the scale of the analysis, irrespective of creep-ductility and grain-boundary configuration of the specimens. The fractal dimension of the grain-boundary fracture was generally larger in specimens with serrated grain boundaries than in specimens with straight grain boundaries in these heat-resistant alloys, because the fractal dimension of the grain boundary and the number of the grain-boundary microcracks were larger in the former specimen. The fractal dimension of the grain-boundary fracture did not tend to converge to unity when the scale of the analysis approached the specimen size. The inclusion of near-specimen size data with regard to the scale of the analysis did not affect the fractal dimension of the grain-boundary fracture in these alloys. Thus, the grain-boundary fracture in the creep-ruptured specimens exhibited a fractal nature, at least in the scale range below specimen size, although there was a cross-over in the fractal dimension of the grain-boundary fracture in specimens containing a large number of grain-boundary microcracks.

1. Introduction

Mandelbrot *et al.* [1] revealed that there is a correlation between the fractal dimension of the fracture surface and the absorbed energy in the impact-loaded and fractured specimens of steels. Similar results were obtained by other investigators in the tensile tests and the fatigue experiments of structural steels [2, 3]. It has recently been found in several heat-resistant alloys of iron-, nickel- and cobalt-base that the improvement of creep-rupture properties by serrated grain boundaries can be correlated with the relative increase in the fractal dimension of the grain boundary (grain-boundary ruggedness) [4]. There is also a correlation between the fractal dimension of the grain boundary, that of the grain-boundary fracture surface profile and the creep-rupture properties in high-temperature creep of metallic materials [5]. It has been reported [6, 7] that the fracture surface may be a self-affine fractal with the local fractal dimension, D, while self-affine surfaces do not have a unique fractal dimension. However, it is still unknown whether there is a unique fractal dimension which characterizes the grain-boundary fracture surface profiles of creep-ruptured specimens in these materials or not.

In this study, the fractal dimension of the grain-boundary fracture in high-temperature creep of heat-resistant alloys was examined in scale ranges of less than and more than about one grain-boundary length by the vertical section method [8, 9]. The box-counting method [10, 11] was employed to estimate the fractal dimension of the grain-boundary fracture including grain-boundary microcracks which were linked to the fracture surface. The effects of inclusion of near-specimen size data with regard to the scale of the analysis on the fractal dimension of the grain-boundary fracture were also examined in this study.

2. Experimental procedure

Table I shows the chemical composition of the heat-resistant alloys used in this study. These alloys were heat-treated to generate serrated or straight grain

0022–2461

TABLE I Chemical composition of the heat-resistant alloys used in this study (wt %)

Alloys	C	N	Cr	Ni	Co	Fe	Mn	Al	Ti	W	Nb	Mo	Si	S	P
HS-21	0.27	B 0.003	26.71	2.37	bal.	0.09	0.64	–	–	–	–	5.42	0.59	0.007	< 0.005
21Cr-4Ni –9Mn steel	0.54	0.39	21.10	4.07	–	bal.	9.74	–	–	–	–	–	0.19	0.008	0.017
L-605	0.07	–	19.82	9.83	bal.	2.22	1.46	–	–	14.37	–	–	0.19	0.002	< 0.005
Inconel X-750	0.06	–	15.03	Ni 71.80	(+Co)	7.48	0.31	1.26	2.43	–	Nb+Ta 1.01	Cu 0.13	0.26	0.001	0.007

TABLE II The heat treatment, the fractal dimension of the grain boundary and the grain size in the heat-resistant alloys

Alloys	Types of grain boundaries	Heat treatment[a]	Fractal dimension of the grain boundary	Grain diameter (μm)
HS-21	Straight	1523 K-3.6 ks → WQ	1.086	130
	Serrated	1523 K-3.6 ks – FC → 1323 K → WQ	1.324	130
21Cr-4Ni -9Mn steel	Straight	1473 K-3.6 ks → WQ + 973 K-108 ks → AC + 1273 K-108 ks → AC	1.108	99
	Serrated	1473 K-3.6 ks → FC → 1303 K → WQ + 1023 K – 108 ks → AC + 1273 K-10.8 ks → AC	1.252	99
L-605	Straight	1473 K-7.2 ks → WQ + 1273 K-1080 ks → AC	1.117	255
	Serrated	1473 K-3.6 ks – FC → 1323 K-72 ks → AC + 1273 K-1080 ks → AC	1.173	260
Inconel X-750	Straight	1423 K-7.2 ks → WQ	1.026	108
	Serrated	1423 K-7.2 ks – FC → 1323 K-21.6 ks → WQ	1.160	125

[a] WQ: water-quenched; AC: air-cooled; FC: furnace-cooled.

boundaries while keeping the matrix strength almost the same in the same alloy. Table II shows the heat treatment, the fractal dimension of the grain boundary and the grain size of specimens in the heat-resistant alloys. The fractal dimension of grain boundaries was determined by the box-counting method [10, 11]. The heat-treated specimens were machined into creep-rupture test pieces of 6 mm diameter and 30 mm gauge length. Creep-rupture experiments were carried out using these specimens with creep-rupture equipment of single-lever type under various stresses in the temperature range 973 K–1422 K. All the test pieces were held for 3.6 ks (Inconel X-750 alloy) or 10.8 ks (other alloys) at each test temperature before loading.

The ruptured specimens were then longitudinally sectioned and the fracture surface profiles were examined by the vertical section method [8, 9] using both optical and scanning electron microscopes. The box-counting method was employed to determine the fractal dimension of the grain-boundary fracture in these alloys [10, 11], because this method was suitable for the estimation of the fractal dimension of the grain-boundary fracture, including grain-boundary microcracks, which were linked to the fracture surface.

Fig. 1 shows a schematic illustration of the box-counting method applied to the analysis of grain-boundary fracture surface profiles in the creep-ruptured specimens. There is a relationship between the number of square boxes, N, intersecting the fracture surface or involving the microcracks linked to the fracture surface, and the side length of a box (the scale of the analysis), r, through the fractal dimension of the grain boundary fracture, D, such that [6, 7].

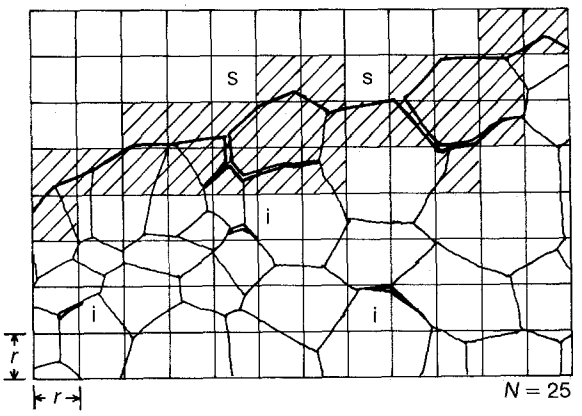

Figure 1 Schematic illustration of the box-counting method applied to the analysis of grain-boundary fracture surface profiles in the creep-ruptured specimens (r = side length of a box, N = number of boxes intersected by the fracture surface profile; s, grain-boundary microcracks linked to the fracture surface; i, isolated grain-boundary microcracks. $N = 25$ in this case).

$$N = F r^{-D} \quad (1)$$

where F is a constant. The actual length of the fracture surface profile, L, is given by the product of N and r, and is expressed as [8, 9].

$$L = L_0 r^{1-D} \quad (2)$$

where L_0 is a constant. The fractal dimension of the grain-boundary fracture was obtained using Equation 2 in this study.

3. Results and discussion

3.1. Specimens containing a large number of grain-boundary microcracks

Table III listed all the data of the fractal dimension of the grain-boundary fracture in ruptured specimens in the heat-resistant alloys. Fig. 2 shows the fractal plot of the fracture surface profile in the specimens of the cobalt-based HS-21 alloys ruptured under a stress of 29.4 MPa at 1311 K. Data points are divided into two groups, which can be fitted to separate straight lines of different slopes, in both the specimen with serrated grain boundaries and that with straight grain boundaries. The fractal dimension of the grain-boundary fracture is larger in the larger scale range of the analysis, r ($D = 1.383$ for the specimen with serrated grain boundaries and $D = 1.332$ for the specimen with straight grain boundaries in the scale range $r > 9 \times 10^{-5}$ m), than in the smaller scale range ($D = 1.227$ for the specimen with serrated grain boundaries and $D = 1.117$ for straight grain boundary in the scale range $r < 9 \times 10^{-5}$ m). The fractal dimension of the grain-boundary fracture is larger in the specimen with serrated grain boundaries than in that with straight grain boundaries when the scale of the analysis r, is less than about one grain-boundary length (9×10^{-5} m), because the fractal dimension of the grain boundary is always larger in the former specimen, even after high-temperature exposure in creep-rupture experiments [5]. However, the difference in the fractal dimension of the grain-boundary fracture is relatively small between these two specimens in the scale range more than about one grain-boundary length, in spite of a large number of the grain-boundary microcracks in the specimen with serrated grain boundaries. Similar results were also obtained in specimens of the same alloy under different creep conditions (Table III).

Fig. 3 shows the microstructures near the fracture surfaces of the specimens shown in Fig. 2. The tensile

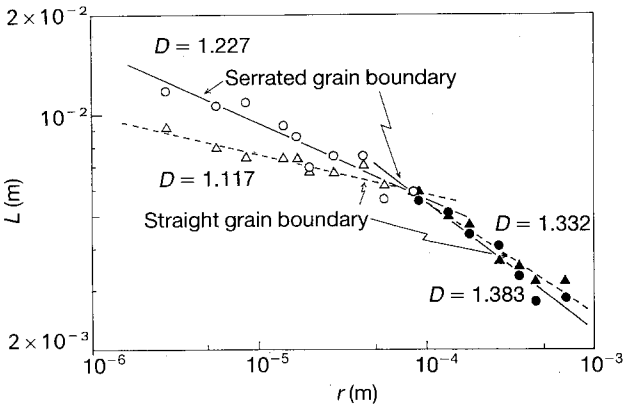

Figure 2 The fractal plot of the fracture surface profile in the specimens of the cobalt-based HS-21 alloy ruptured under a stress of 29.4 MPa at 1311 K. D = fractal dimension.

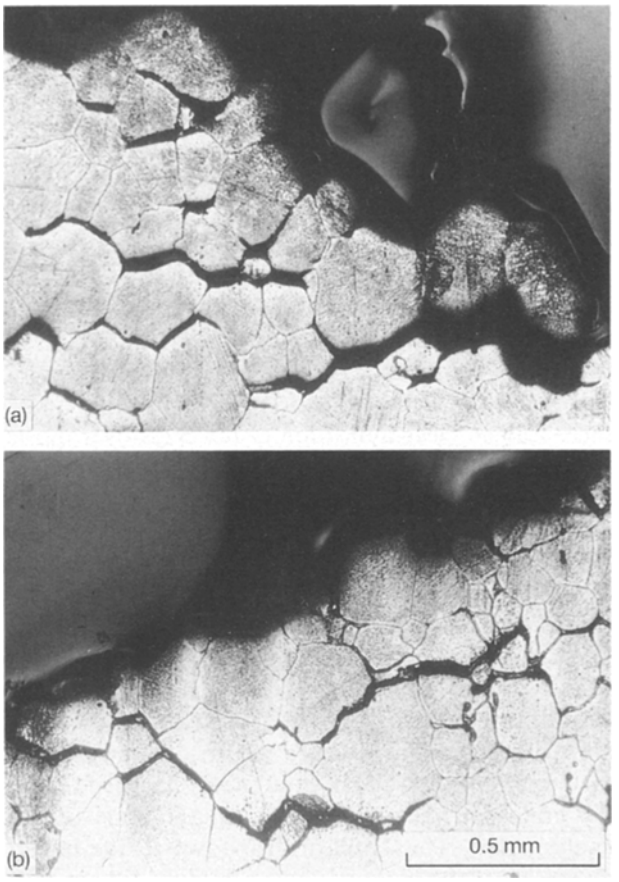

Figure 3 The microstructures near the fracture surfaces in the specimens of the HS-21 alloy ruptured under a stress of 29.4 MPa at 1311 K. (a) Specimen with serrated grain boundaries (t_r = 395.6 ks, ε_r = 0.0563); (b) specimen with straight grain boundaries (t_r = 226.6 ks, ε_r = 0.0276). t_r = rupture life; ε_r = elongation.

TABLE III The fractal dimension of the grain-boundary fracture in the heat-resistant alloys

Alloys	Creep conditions (K)	(MPa)	Grain-boundary configuration	Fractal dimension (side length of boxes in box-counting method, m)	
HS-21	1089	137	Serrated	1.222 (5.62×10^{-7}–6.74×10^{-5})	1.292 (8.90×10^{-5}–6.68×10^{-4})
			Straight	1.142 (5.62×10^{-7}–6.74×10^{-5})	1.217 (8.90×10^{-5}–6.68×10^{-4})
	1311	29.4	Serrated	1.227 (2.81×10^{-7}–8.42×10^{-5})	1.383 (8.90×10^{-5}–6.68×10^{-4})
			Straight	1.117 (2.81×10^{-7}–8.42×10^{-5})	1.332 (8.90×10^{-5}–6.68×10^{-4})
	1422	19.6	Serrated	1.137 (5.62×10^{-7}–6.74×10^{-5})	1.380 (8.90×10^{-5}–6.68×10^{-4})
			Straight	1.136 (5.62×10^{-7}–6.74×10^{-5})	1.384 (8.90×10^{-5}–6.68×10^{-4})
L-605	1089	137	Serrated	1.170 (2.81×10^{-7}–8.42×10^{-5})	1.198 (8.90×10^{-5}–6.68×10^{-4})
			Straight	1.151 (2.81×10^{-7}–8.42×10^{-5})	1.174 (8.90×10^{-5}–6.68×10^{-4})
Inconel X-750	973	294	Serrated	1.218 (5.62×10^{-7}–3.37×10^{-5})	1.198 (6.68×10^{-5}–4.45×10^{-4})
			Straight	1.173 (5.62×10^{-7}–3.37×10^{-5})	1.140 (6.68×10^{-5}–4.45×10^{-4})
21Cr–4Ni–9Mn steel	973	196	Serrated	1.241 (2.81×10^{-6}–5.62×10^{-5})	1.259 (5.67×10^{-5}–4.25×10^{-4})
			Straight	1.207 (2.81×10^{-6}–5.62×10^{-5})	1.243 (5.67×10^{-5}–4.25×10^{-4})

direction is vertical in the micrographs. Creep-rupture properties of these specimens are also given in the caption. Many grain-boundary microcracks, which are linked to the fracture surface, are visible in both the specimen with serrated grain boundaries (Fig. 3a) and that with straight grain boundaries (Fig. 3b), whereas the number of these microcracks is somewhat larger in the former specimen. Thus, the larger value of the fractal dimension of the grain-boundary fracture in the larger scale range ($r > 9 \times 10^{-5}$ m) reflects that the grain-boundary microcracks linked to the fracture surface are taken into account in the estimation of the fractal dimension of the grain-boundary fracture. Similar results were obtained in the ruptured specimens of 21Cr–4Ni–9Mn steel (Table III), but there was only a small difference in the fractal dimension of the grain-boundary fracture between the two scale ranges of the analysis because of the relatively small number of grain-boundary microcracks in this steel.

3.2. Specimens with a very small number of grain-boundary microcracks

In the alloys containing a much fewer number of grain-boundary microcracks with larger rupture ductility, there was no clear indication of the cross-over in the length scale. Fig. 4 shows the fractal plot for specimens of the cobalt-based L-605 (HS-25) alloy ruptured under a stress of 118 MPa at 1089 K. Extensive creep deformation occurred in the interior of the grains in this alloy, irrespective of grain-boundary configuration of the specimens. Fig. 5 shows an example of the fracture surface profile of the ruptured specimen with serrated grain boundaries. The tensile direction is vertical in the micrographs. Plastic deformation in the matrix (in the grains) affected the fractal dimension of the grain-boundary [5, 12] and then influenced that of the grain-boundary fracture in all the scale ranges analysed [5]. Thus, a clear cross-over in the fractal dimension of the grain-boundary fracture did not exist in this alloy. The fractal dimension of the grain-boundary fracture is larger in the specimen with serrated grain boundaries than in that with straight grain boundaries, because the fractal dimension of the grain boundary is larger in the former specimen (Table II).

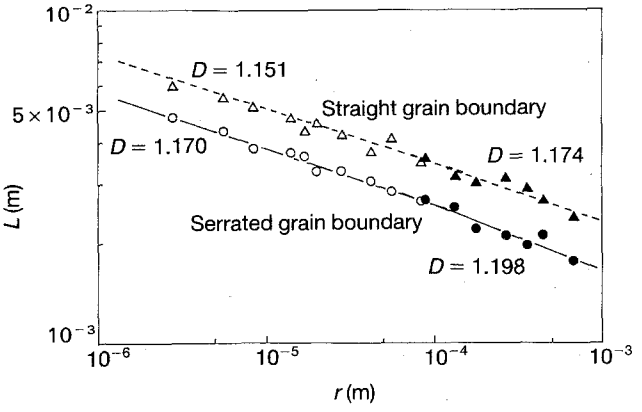

Figure 4 The fractal plot of the fracture surface profile in the specimens of the cobalt-based L-605 (HS-25) alloy ruptured under a stress of 137 MPa at 1089 K.

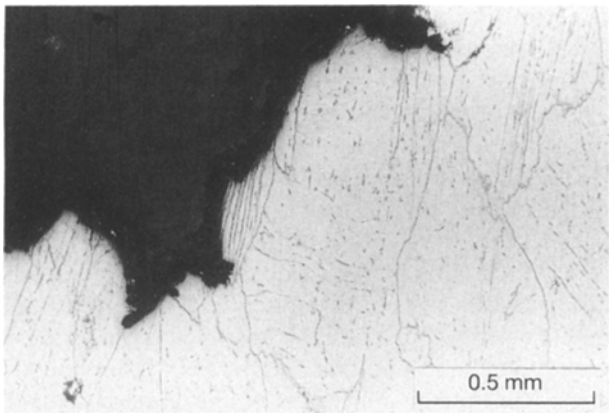

Figure 5 The fracture surface profile in the specimen with serrated grain boundaries of the L-605 alloy ruptured under a stress of 137 MPa at 1089 K ($t_r = 779.6$ ks, $\varepsilon_r = 0.311$).

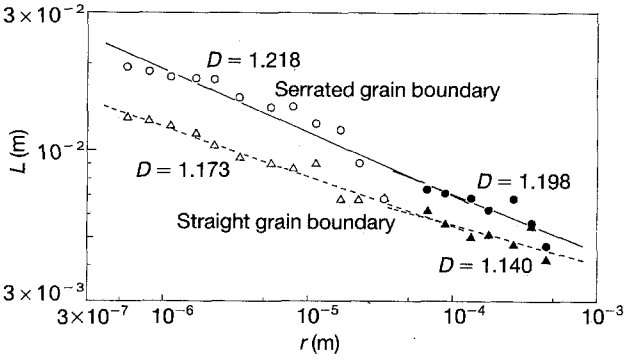

Figure 6 The fractal plot of the fracture surface profile in the specimens of the nickel-based Inconel X-750 alloy ruptured under a stress of 294 MPa at 973 K.

There was also no clear cross-over in the fractal dimension of the grain-boundary fracture with regard to the scale of the analysis in alloys with very low ductility and a very small number of grain-boundary microcracks. Fig. 6 shows the fractal plot in the specimens of the nickel-based Inconel X-750 alloy ruptured under a stress of 294 MPa at 973 K. The fractal dimension of the grain-boundary fracture changes from a slightly larger value in the scale range less than one grain-boundary length (about 7×10^{-5} m) to a smaller value in the scale range more than one grain-boundary length, and these values are larger in the specimen with serrated grain boundaries. Fig. 7 shows a fracture surface profile of the ruptured specimen with straight grain boundaries. The tensile direction is vertical in the micrographs. It is conceivable that the grain-boundary fracture surface exhibits an affine nature in this kind of alloy when the specimen size or the scale of the analysis becomes very large [6, 7]. However, as will be shown later, inclusion of the near-specimen size data with regard to the scale of the analysis did not affect the fractal dimension of the grain-boundary fracture in high-temperature creep of heat-resistant alloys.

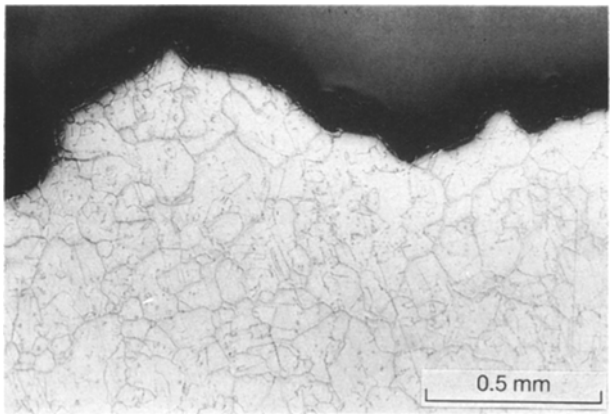

Figure 7 The fracture surface profile in the specimen with straight grain boundaries of the Inconel X-750 alloy ruptured under a stress of 294 MPa at 973 K (t_r = 1605 ks, ε_r = 0.006 67).

3.3. Inclusion of near-specimen size data to determination of fractal dimension of grain-boundary fracture

It has been reported that the fracture surface may be a self-affine fractal which does not have a unique fractal dimension [6, 7]. However, in high-temperature creep of heat-resistant alloys in this study, the fractal dimension of the grain-boundary fracture did not tend to converge to unity when the scale of the analysis approached specimen size.

Fig. 8 shows the fractal plot in the scale range between one grain-boundary length and the specimen size (about 4×10^{-3} m) on several creep-ruptured specimens of the heat-resistant alloys. Each data set can be fitted to a single straight line in $\log_{10} L$–$\log_{10} r$ plot, and the slope of this line is very close to the value of the fractal dimension of the grain-boundary fracture in the scale range more than one grain-boundary length (Figs 2, 4 and 6, Table III), irrespective of grain-boundary configuration and creep-ductility of the specimens. The same results were also obtained on other

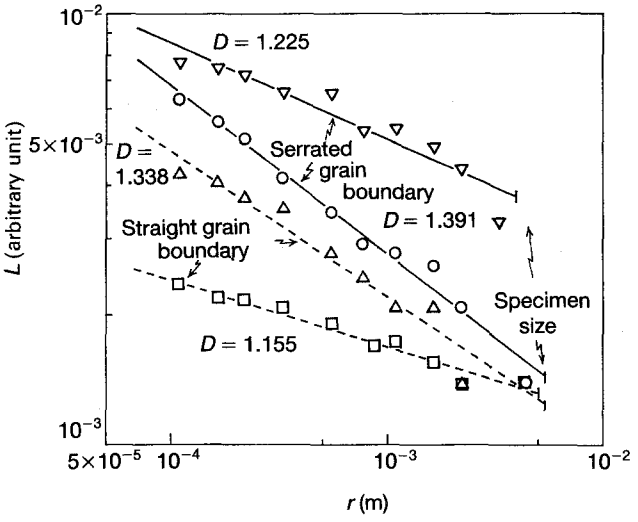

Figure 8 The fractal plot of the fracture surface profile in the specimens of the heat-resistant alloys in the scale range between about one grain-boundary length and the specimen size (▽) L-605, 1089 K, 137 MPa; (○, △) HS-21, 1311 K, 29.4 MPa; (□) Inconel X-750, 973 K, 294 MPa.

heat-resistant alloys. Thus, the grain-boundary fracture surfaces have a fractal nature in creep fracture at least in the scale range less than the specimen size, although the fractal dimension of the grain-boundary fracture has a cross-over in the scale of the analysis in specimens containing a large number of grain-boundary microcracks.

4. Conclusions

The fractal dimension of the grain-boundary fracture in high-temperature creep was estimated by the vertical section method on several creep-ruptured specimens of cobalt-, nickel- and iron-based heat-resistant alloys. The results obtained are summarized as follows.

1. In specimens containing many grain-boundary microcracks linked to the fracture surface, there was a cross-over in the fractal dimension of the grain-boundary fracture at about one grain-boundary length. The fractal dimension of the grain-boundary fracture estimated in the scale range of more than about one grain-boundary length, was a little larger than that obtained in the scale range less than this length.

2. In specimens containing much fewer microcracks, there was no clear cross-over in the fractal dimension of the grain-boundary fracture with regard to the scale of the analysis, irrespective of creep ductility and grain-boundary configuration of the specimens.

3. The fractal dimension of the grain-boundary fracture was generally larger in the specimen with serrated grain boundaries than in the specimen with straight grain boundaries of the same alloy, because the fractal dimension of the grain boundary was larger in the former specimen than in the latter. However, the difference in the fractal dimensions between these specimens was smaller in the scale range of more than about one grain-boundary length, in spite of a relatively large number of grain-boundary microcracks in the former specimen.

4. Inclusion of the near-specimen size data with regard to the scale of the analysis did not affect the value of the fractal dimension of the grain-boundary fracture in the scale range of more than about one grain-boundary length. Thus, the fractal dimension of the grain-boundary fracture in creep-ruptured specimens had a fractal nature at least in the scale range of less than specimen size (about 4×10^{-3} m).

References

1. B. B. MANDELBROT, D. E. PASSOJA and A. J. PAULLAY, *Nature* **308** (1984) 721.
2. E. E. UNDERWOOD and K. BANERJI, *Mater. Sci. Eng.* **80** (1986) 1.
3. Z. G. WANG, D. L. CHEN, X. X. JIANG, S. H. AI and C. H. SHIH, *Scripta Metall.* **22** (1988) 827.
4. M. TANAKA and H. IIZUKA, *Z. Metallkde* **82** (1991) 442.
5. M. TANAKA, *J. Mater. Sci.* **27** (1992) 4717.
6. B. B. MANDELBROT, "Dynamics of Fractal Surfaces", edited by F. FAMILY and T. VICSEK (World Scientific, Singapore, 1991) p. 5.

7. J. FEDER, in "Fractals", translated by M. MATSUSHITA, Y. HAYAKAWA and S. SAITO (Keigakukan, Tokyo, 1991) p. 245.
8. C. S. PANDE, L. E. RICHARDS, N. LOUAT, B. D. DEMPSEY and A. J. SCHWOEBLE, *Acta Metall.* **35** (1987) 1633.
9. K. BANERJI, *Met. Trans.* **19A** (1988) 961.
10. S. ISHIMURA and S. ISHIMURA, "Fractal Mathematics" (Tokyo Tosho, Tokyo, 1990) p. 246.
11. H. TAKAYASU, "Fractals in the Physical Sciences", (Manchester University Press, Manchester, New York, 1990) p. 11.
12. E. HORNBOGEN, *Z. Metallkde* **78** (1987) 622.

Received 18 May 1992
and accepted 5 March 1993